Photoacoustic oxygenation imaging to identify ischemia/hypoxia injury and necrosis of intestine after acute intussusception: A comparative study with CDFI/CEUS

Hualin Yan [a,b], Zehui Gou [a,b], Hong Wang [a,b], Xiaoxia Zhu [a,b], Juxian Liu [a], Wenwu Ling [a,b], Lin Huang [c,*], Yan Luo [a,b,**]

[a] Department of Medical Ultrasound, West China Hospital, Sichuan University, Chengdu 610041, China
[b] Tianfu Jincheng Laboratory, City of Future Medicine, Chengdu 641400, China
[c] School of Electronic Science and Engineering, University of Electronic Science and Technology of China, Chengdu 611731, China

ARTICLE INFO

ABSTRACT

Acute intussusception is a pediatric abdominal emergency that requires immediate diagnosis and treatment. However, accurately identifying bowel necrosis non-invasively remains challenging with conventional sonography. In our study, we investigated the potential of photoacoustic imaging (PAI) as an innovative method for assessing ischemia/hypoxia injury and intestinal necrosis in cases of acute intussusception. Using PAI, we measured intestinal oxygen saturation (sO_2) levels and total hemoglobin (HbT) in various models of acute intussusception at different time points. Additionally, we evaluated blood supply and ischemia/hypoxia injury using color Doppler flow imaging (CDFI) and contrast-enhanced ultrasound (CEUS). Based on histopathological results, intestinal sO_2 measured by PAI demonstrated optimal diagnostic performance for both ischemia/hypoxia injury and intestinal necrosis, with AUC values of 0.997 and 0.982, respectively, while CDFI and CEUS showed relatively high diagnostic performance for both ischemia/hypoxia injury and intestinal necrosis. In conclusion, PAI represents a promising, non-invasive imaging modality for assessing acute intussusception.

1. Introduction

Acute intussusception is one of the most common abdominal emergencies in children under three years of age, characterized by the invagination of the proximal bowel into the distal bowel. The incidence of acute intussusception is approximately 5 per 10,000 infants annually [1,2]. The most prevalent form of this condition is idiopathic ileocolic intussusception, which leads to strangulating intestinal obstruction and mesenteric ischemia, necessitating the reduction of the intussusception. Non-operative enema (either air or liquid) is the preferred method of reduction for most cases of idiopathic ileocolic intussusception, with an overall success rate of 76.8 % [1]. However, bowel necrosis and perforation are the contraindications for enema reduction, requiring emergency surgery [2]. Nevertheless, accurately identifying bowel necrosis in acute intussusception non-invasively remains a challenge. The missed diagnosis or misdiagnosis of bowel necrosis would lead to failure of enema reduction or unnecessary surgery.

Non-invasive ultrasound (US) is the first-choice imaging modality to diagnose acute intussusception at most institutions, offering 97 % sensitivity and 98 % specificity in diagnosis [3,4]. However, it is hard to identify bowel necrosis through conventional ultrasound. Although the absence of blood flow on color Doppler ultrasound suggests bowel ischemia and is associated with a lower success rate of reduction, it does not serve as an absolute contraindication for enema reduction, as there are cases where reduction still succeeds [5,6]. On the other hand, no blood flow on color Doppler may be late in the diagnosis of intestinal necrosis [7]. Similarly, the presence of trapped peritoneal fluid between two limbs of the intussusceptum on ultrasound is also associated with a lower reduction success rate and a higher degree of bowel ischemia [8,9]. However, this sonographic sign is also not considered a contraindication for enema reduction [2,10]. Thus, a more accurate non-invasive method is urgently needed to identify bowel necrosis and prevent misdiagnosis or missed diagnosis.

Photoacoustic imaging (PAI) is an innovative hybrid imaging

---

* Corresponding author.
** Corresponding author at: Department of Medical Ultrasound, West China Hospital, Sichuan University, Chengdu 610041, China.
E-mail addresses: lhuang@uestc.edu.cn (L. Huang), yanluo@scu.edu.cn (Y. Luo).

modality that combines optical imaging contrast with ultrasonic high spatial resolution. By leveraging the distinct absorption spectra of oxygenated and deoxygenated hemoglobin using dual-wavelength PAI, it is possible to quantify tissue oxygen saturation (sO_2) and total hemoglobin (HbT) counts, which have been demonstrated useful in diagnosing and monitoring diseases associated with hypoxia, ischemia and inflammation [11–13]. In our previous study, we demonstrated that PAI possesses excellent diagnostic capabilities in detecting testicular torsion (TT) and identifying ischemia/hypoxia injuries following testicular torsion [14]. Intestinal ischemia/hypoxia injury is a consequence of acute intussusception, caused by strangulating intestinal obstruction, which can progress to bowel necrosis if severe [15]. Therefore, monitoring and measuring intestinal sO_2 and HbT following acute intussusception may assist in identifying severe ischemia/hypoxia injuries and potential bowel necrosis.

This study aimed to investigate the feasibility of using PAI to detect early and late stages of intestinal ischemia/hypoxia injury following acute intussusception, and attempt to identify severe intestinal ischemia/hypoxia injury and necrosis based on PAI, using histopathological assessments of injury degree as the gold standard.

2. Methods

2.1. Animals

A total of 32 male New Zealand rabbits, weighing between 2.2 and 3.0 kg, were provided and housed under standard living conditions for a 2-week acclimatization period. All animal experiments were conducted in compliance with the National Institutes of Health Guide for the Care and Use of Laboratory Animals and were approved by the Animal Care and Use Committee of West China Hospital.

2.2. Acute intussusception modeling

Surgery was performed on the rabbits after anesthesia was induced with an intramuscular injection of Zoletil™ (Virbac corporation, TX, USA) at a dosage of 5 mg/kg, followed by an intraperitoneal administration of 1 % pentobarbital sodium at a dosage of 3 ml/kg. Prior to surgery, the abdominal region was shaved and sterilized. Acute intussusception modeling was established following a previously described method [16], summarized as follows: First, laparotomy was performed, and the small intestine was freed. Next, the terminal 10–15 cm of the ileum was intussuscepted into the colon using a Kirschner wire. Finally, the intussusception was secured with a tension-free suture of the colon's serosal layer. In the sham operation group (Group S; n = 10), only laparotomy was performed without inducing intussusception. Immediately after acute intussusception, a subset of rabbits (randomly selected) was examined by US to validate the intussusception and then assessed with CDFI, CEUS for blood supply assessment, and photoacoustic imaging (PAI) for sO_2 and HbT detection (Group A; n = 10). Two hours after acute intussusception, another subset of rabbits (randomly selected) was examined by US to validate the intussusception and then assessed with CDFI, CEUS for blood supply assessment, and PAI for sO_2 and HbT detection (Group B; n = 10). Eight hours after acute intussusception, a third subset of rabbits (randomly selected) was examined by US to validate the intussusception and then assessed with CDFI, CEUS for blood supply assessment, and PAI for sO_2 and HbT detection (Group C; n = 10). All animals were sacrificed immediately after PAI, and the intussuscepted intestinal specimens were surgically removed, washed twice with normal saline, and fixed in 10 % formaldehyde for histological analysis.

2.3. CDFI and Adler grade classification

B-mode US and CDFI examinations were performed by an experienced operator (Z.G.) using a multi-modal ultrasound system (Mindray

Resona 7, Shenzhen, China) equipped with an L14–5 transducer (5–14 Hz). Blood flow classification based on the Adler grading criteria [17] as follows: Grade 0: no blood flow within the lesion; Grade 1: one or two pixels of blood flow (typically <1 mm in diameter) observed within the lesion; Grade 2: three to four pixels or a main vessel visualized within the lesion; Grade 3: more than four pixel-sized vessels visualized or vessels forming an intertwined network within the lesion.

2.4. CEUS and time-intensity curve analysis

CEUS was performed by an experienced operator (Z.G.) using a multi-modal ultrasound system (Mindray Resona 7, Shenzhen, China) with an L14–5 (5–14 Hz) transducer. A bolus of 1–1.5 ml i.v. of sulfur-hexafluoride microbubbles (SonoVue®, Bracco, Italy), followed by a 5 ml saline flush, was administered via the ear vein. At least 60 seconds of video was recorded for time-intensity curve (TIC) analysis. The primary parameters analyzed of TIC included the area under the curve (AUC), time to peak (TTP), peak intensity (PI), and mean transit time (MTT).

2.5. Photoacoustic imaging system and data acquisition

As illustrated in Fig. 1, US and PAI were acquired using a VEVO LAZR High-Resolution Ultrasound and Photoacoustic Imaging System (FUJIFILM VisualSonics, Inc., Toronto, ON, Canada), as described previously [11,18]. Briefly, Animals were placed supine on a heated imaging stage with continuous physiological monitoring. A 256-element linear-array transducer MX250, with frequency of 21 MHz, was used to image in the sagittal plane with centrifuged ultrasound gel to provide acoustic coupling. The VEVO LAZR system utilizes a Nd:YAG laser with an optical parametric oscillator, tunable in the near-infrared (NIR) range of 680–970 nm with 20 Hz repetition rate.

For imaging tissue oxygenation (sO_2), the VEVO Oxy-Hemo imaging mode was employed to measure the PA signal at spectral wavelengths of 750 nm and 850 nm. The calculation of sO_2 is automated within the VEVO LAZR system, based on the ratio of oxyhemoglobin to total hemoglobin. sO_2 images were recorded for subsequent oxygenation analysis, with an acquisition rate of 1 frame per second. Different planes in one animal were captured. The data were averaged over time for consecutive frames in a plane.

To measure the total hemoglobin (HbT) per mm^2 within the involved intestines, all detected signals at the two wavelengths (750 nm and 850 nm) were divided by the intestinal area [11,19]. Imaging parameters were kept constant between animals. Quantitative analysis of US and PAI results was performed by using the VEVO LAB 1.7.2. software (FUJIFILM VisualSonics Inc.). The region of interests (ROIs) for both the intussusceptum (the proximal segment that invaginates into the distal segment, typically the ileum and sacculus rotundus [the terminal end of a rabbit's ileum]) and intussuscipiens (the recipient distal segment, typically the colon) was manually defined over the involved intestinal region. An average value of tissue sO_2 within this intestinal ROI was extracted as a measure of intestinal tissue oxygenation and an average value of tissue HbT counts/mm^2 within this intestinal ROI was extracted as a measure of HbT per mm^2.

2.6. Histopathological assessment

The intussuscepted intestinal specimens were surgically removed immediately after PAI. The excised tissues underwent histological examination using hematoxylin and eosin (H&E) staining and immunohistochemical (IHC) staining with HIF-1α. Microscopic images of the stained tissues were captured using an Axio Imager.A2 microscope (Carl Zeiss Microscopy, NY, USA).

Based on the histopathological changes, the involved intestines were evaluated using Chiu's histological grading criteria and classified as follows: grade 0, normal; grade 1, subepithelial edema, partial
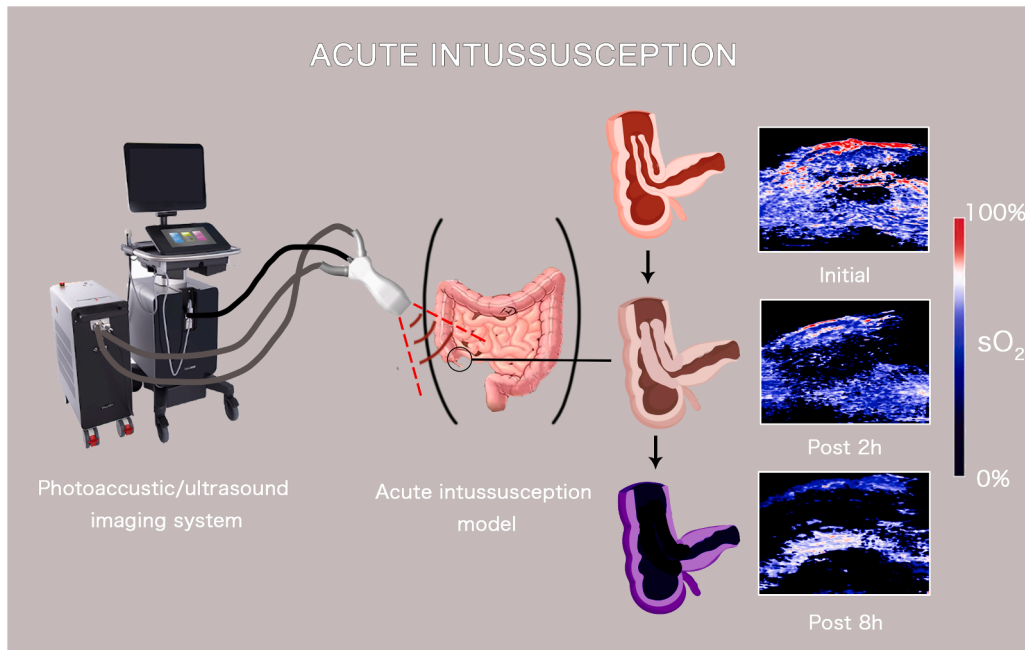
Fig. 1. Schematic diagram for photoacoustic imaging of acute intussusception.

separation of apical cells; grade 2, epithelial cell slough from the tips of villi; grade 3, progression of slough to the base of villi; grade 4, partial mucosal necrosis of the lamina propria; grade 5, total mucosal necrosis [20,21].

The degree of HIF-1α expression, indicative of hypoxic conditions, was evaluated for each histological section using a scoring system ranging from 1 to 3 [14]. This scoring was determined by both the expression rate and staining intensity. Cases exhibiting no or mild staining and an expression rate below 30 % were assigned a score of 1. Cases with moderate staining and an expression rate between 30 % and 70 % were given a score of 2, while cases demonstrating intense staining and an expression rate exceeding 70 % were scored as 3.

2.7. Statistical analysis

SPSS 25.0 (IBM Corp., Armonk, NY, USA) and MedCalc 10.4 (Med-Calc Software Ltd, Ostend,Belgium) software was used for statistical analysis. One-way ANOVA was used to compare the TIC parameters, PAI measurements of sO_2 among different groups after confirming normality, with Bonferroni correction applied for multiple comparisons. The Kruskal-Wallis test was used to compare ranked variables, such as the Adler grades, the Chiu grades, and HIF-1α score, also with Bonferroni correction for multiple comparisons. The diagnostic performance of HbT counts and sO_2 in the diagnosis of acute intussusception, particularly in identifying pathological ischemia/hypoxia injury and intestinal necrosis, was assessed by calculating the areas under the receiver operating characteristic (ROC) curves (AUCs) with 95 % confidence intervals (CIs). The cutoff value was determined by the highest Youden index. Comparisons of different AUCs were performed using DeLong's test. The corresponding sensitivity, specificity, and accuracy of the HbT counts and sO_2 were calculated. All tests were two-tailed, and a *P*-value < 0.05 was considered statistically significant.

3. Results

3.1. Workflow of normal intestine and injured intestine in acute intussusception

A timeline illustrating the workflow and defining the different

groups is presented in Fig. 2. Following the onset of acute intussusception, strangulating intestinal ischemia progressively intensifies, ultimately resulting in the gradual destruction of the histological structure of the intestinal wall. Blood supply to the intestines was evaluated using CDFI and CEUS, while sO_2 and HbT levels were analyzed over time using PAI. A comprehensive quantitative analysis of all measurements across different groups was performed.

3.2. Changes of sO_2 and HbT detected by PAI

Representative macroscopic photographs of each group, along with corresponding B-mode US images, PAI of sO_2, and PAI of HbT, are shown in Fig. 3. Macroscopic examination revealed pronounced congestion and swelling in the intussusceptum of group B (white arrow, Fig. 3c$_1$) and evident bluish discoloration and swelling in group C (white arrow, Fig. 3d$_1$).
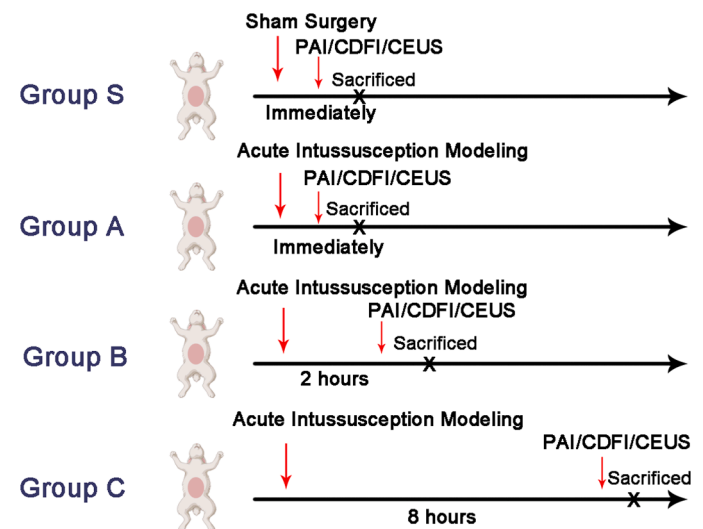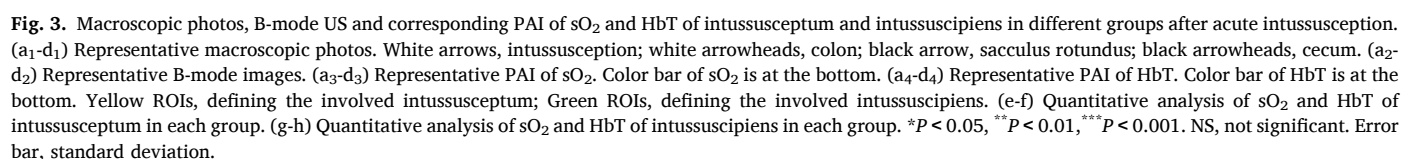

Fig. 2. The timeline diagram illustrating the workflow and defining the different groups. CDFI, color flowing imaging; CEUS, contrast-enhanced ultrasound; PAI, photoacoustic imaging.

Fig. 3. Macroscopic photos, B-mode US and corresponding PAI of sO$_2$ and HbT of intussusceptum and intussuscipiens in different groups after acute intussusception. (a$_1$-d$_1$) Representative macroscopic photos. White arrows, intussusception; white arrowheads, colon; black arrow, sacculus rotundus; black arrowheads, cecum. (a$_2$-d$_2$) Representative B-mode images. (a$_3$-d$_3$) Representative PAI of sO$_2$. Color bar of sO$_2$ is at the bottom. (a$_4$-d$_4$) Representative PAI of HbT. Color bar of HbT is at the bottom. Yellow ROIs, defining the involved intussusceptum; Green ROIs, defining the involved intussuscipiens. (e-f) Quantitative analysis of sO$_2$ and HbT of intussusceptum in each group. (g-h) Quantitative analysis of sO$_2$ and HbT of intussuscipiens in each group. *$P < 0.05$, **$P < 0.01$, ***$P < 0.001$. NS, not significant. Error bar, standard deviation.

Compared to the controls (group S), the sO_2 levels in the affected intussusceptum of group A remained relatively unchanged (72.97 ± 9.08 % vs. 73.84 ± 6.53 %, Table 1, Fig. 3, $P = 1.000$). However, two hours after acute intussusception, the sO_2 levels in group B (56.52 ± 6.23 %) were significantly reduced compared to both group S (73.84 ± 6.53 %) and group A (72.97 ± 9.08 %) (Table 1, Fig. 3e, both $P <$ 0.001). Moreover, eight hours after the onset, the sO_2 levels in group C (45.28 ± 3.50 %) were significantly lower than those in group S (73.84 ± 6.53 %), group A (72.97 ± 9.08 %), and group B (56.52 ± 6.23 %) (Table 1, Fig. 3e, $P < 0.001$, $P < 0.001$, and $P = 0.003$, respectively). However, the sO_2 levels in the intussuscipiens exhibited a slower decline, with a significant reduction observed only in group C (40.49 ± 9.05 %) compared to group S (75.09 ± 5.52 %), group A (74.38 ± 9.39 %), and group B (66.26 ± 11.71 %) (Table 1, Fig. 3g, all $P < 0.001$). These results are consistent with the clinical experience that the intussusceptum is the most vulnerable and first to experience hypoxia and necrosis.

As acute intussusception led to strangulating intestinal ischemia, the total hemoglobin (HbT) counts decreased over time. Compared to the initial group A (44,489 ± 20,856 /mm^2), the HbT counts per mm^2 of the affected intussusceptum in group B (17,344 ± 7,125 /mm^2) and group C (22,442 ± 13,149 /mm^2) were significantly lower (Table 1, Fig. 3f, $P = 0.027$ and $P = 0.045$, respectively). However, no significant differences in HbT counts were found between group B and group C ($P = 0.614$). Similarly, the HbT counts per mm^2 in groups B and C were significantly lower compared to the sham group (45,558 ± 34,688/ mm^2) (Table 1, Fig. 3f, $P = 0.015$ and $P = 0.023$, respectively). The significant decrease of HbT indicated the remarkable ischemia of the affected intussusceptum in group B and group C. However, no significant changes in HbT counts were observed in the intussuscipiens (Fig. 3h).

3.3. Changes in blood supply evaluated by CDFI and CEUS

Representative CDFI images for each group, along with corresponding B-mode and CEUS images, are shown in Fig. 4. At the initial stage of intussusception (group A), no evidence of significant ischemia was observed in the intussusceptum on either CDFI or CEUS images (arrows, Figs. 4b$_1$ and 4b$_2$). However, two hours (group B) and eight hours (group C) after the onset of intussusception, marked ischemia was evident in the intussusceptum in both CDFI and CEUS images (arrows, Figs. 4c$_1$, 4c$_2$, 4d$_1$, and 4d$_2$).

Quantitative analysis showed that, compared to the control group (group S, median: Adler grade 2) and the initial group (group A, median: Adler grade 2), the CDFI Adler grade was significantly lower in groups B and C (median: Adler grade 0.5) (Fig. 4e, all $P < 0.05$), which means the remarkable ischemia in the intussusceptum of groups B and C. TIC analysis of CEUS revealed significantly reduced AUC values in groups B and C compared to groups S and A (Fig. 4f, all $P < 0.05$). Similarly, PI values were significantly lower in group C compared to groups S and A (Fig. 4g, both $P < 0.001$). TTP values were significantly prolonged in groups B and C compared to groups S and A (Fig. 4h, all $P < 0.05$). MTT was extended only in group C compared to group A (Fig. 4i, $P = 0.019$). The decline in AUC and PI values, along with the extension of TTP and MTT, indicates a sustained deterioration in blood supply to the intussusceptum in both groups B and C.

3.4. Histopathology and immunohistochemistry changes

The intestines in group S and group A exhibited normal villi without any structural damage (Fig. 5a$_1$ and 5b$_1$). In contrast, histological analysis of group B revealed marked epithelial lifting along the sides of the villi, with some tips denuded (Fig. 5c$_1$). In group C, the lamina propria was severely compromised, showing signs of destruction, digestion, and disintegration, accompanied by significant hemorrhage and ulceration (Fig. 5d$_1$). When graded according to Chiu's criteria, the grades in group C (median: grade 4.5) were significantly higher than those in group S (median: grade 0), group A (median: grade 0), and group B (median: grade 2) (Fig. 5e, all $P < 0.001$). The Chiu's grades in group B were also higher than those in group S and group A (Fig. 5e, $P = 0.006$ and $P = 0.006$, respectively). Histopathological examination confirmed ischemia/hypoxia injury in group B (median: grade 2, range: 1–3) and necrotic intestinal damage in group C (median: grade 4.5, range: 4–5). No significant changes in Chiu's grade were observed between group S and group A ($P = 1.000$).

HIF-1α was scarcely expressed in normal intestinal tissue (Fig. 5a$_2$). However, following acute intussusception, the expression of HIF-1α increased over time, as shown in Fig. 5b$_2$-d$_2$. In group C, the expression levels of HIF-1α in group C (median: Hif-1α score 2) were significantly increased compared to those in group S (median: Hif-1α score 1), group A (median: Hif-1α score 1) and group B (median: Hif-1α score 1.5) (Fig. 5f, $P = 0.001$, $P = 0.001$ and $P = 0.037$, respectively). Hif-1α was overexpressed under hypoxia condition and would lead to apoptosis and cell death [22]. The results demonstrated the serve hypoxia condition of group C.

3.5. Diagnostic performance of CDFI, CEUS and PAI in identifying ischemia/ hypoxia injury of intestine after acute intussusception

Regarding the pathological changes that occur after acute intussusception, ischemia/ hypoxia injury of intestine was defined as the Chiu's grade above 2. Based on this classification, the CDFI Adler grade demonstrated relatively high diagnostic performance in identifying intestinal ischemia/hypoxia injury, with an AUC of 0.896 (95 % CI: 0.729–0.977, Table 2, Fig. 6a), with a sensitivity of 89 %, specificity of

Table 1

The mean oxygen saturation (sO_2) and HbT counts of intussusceptum and intussuscipiens in different groups after acute intussusception.

Groups	sO_2 of intussusceptum (%)[a]	HbT of intussusceptum (counts)[a]	sO_2 of intussuscipiens (%)[a]	HbT of intussuscipiens (counts)[a]
Group S	73.84 ± 6.53	45,558 ± 34,688	75.09 ± 5.52	50,254 ± 34,612
Group A	72.97 ± 9.08	44,489 ± 20,856	74.38 ± 9.39	51,056 ± 14,840
Group B	56.52 ± 6.23[***, †††]	17,344 ± 7,125[*, †]	66.26 ± 11.71	46,140 ± 18,678
Group C	45.28 ± 3.50[***, †††, §]	22,442 ± 13,149[*, †]	40.49 ± 9.05[***, †††, §§§]	48,702 ± 20,067

HbT, total hemoglobin.
[a] data are mean ± standard deviation.
*compared to group S. < 0.05
**compared to group S. < 0.01,
***compared to group S. < 0.001.
†compared to group A. < 0.05,
††compared to group A. < 0.01,
†††compared to group A. < 0.001.
§compared to group B. < 0.05,
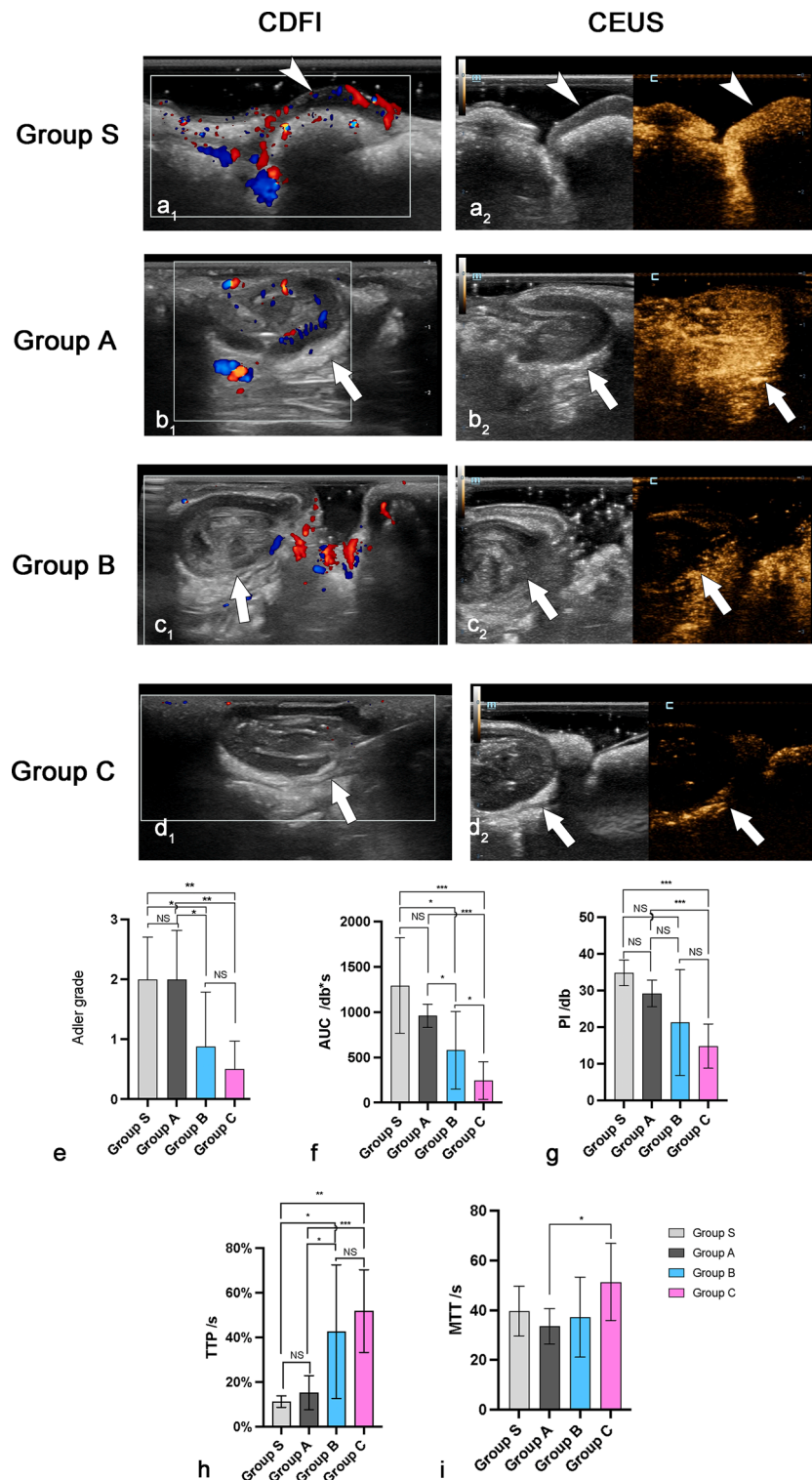§compared to group B. < 0.01,
§§§compared to group B. < 0.001.

Fig. 4. CDFI and corresponding CEUS images in different groups after acute intussusception. (a_1-d_1) Representative CDFI images. (a_2-d_2) Representative CEUS images. (e) Alder grade analysis of different groups. White arrows, intussusception; white arrowhead, sacculus rotundus. (f-i) Time-intensity curve analyses of different groups. AUC, the area under the curve; CDFI, color flowing imaging; CEUS, contrast-enhanced ultrasound; MTT, mean transit time; PI, peak intensity; TTP, time to peak. *$P < 0.05$, **$P < 0.01$, ***$P < 0.001$. NS, not significant. Error bar, standard deviation.

75 %, and accuracy of 83 %. Among all the TIC parameters, the AUC of CEUS exhibited superior diagnostic performance, achieving an AUC of 0.939 (95 % CI: 0.784–0.994, Table 2, Fig. 6a), with a sensitivity of 94 %, specificity of 91 %, and accuracy of 93 %. These findings suggest that both CDFI and CEUS demonstrate high diagnostic accuracy in detecting ischemia and hypoxia-induced injury in the intestine

following acute intussusception.

Photoacoustic imaging (PAI) demonstrated outstanding diagnostic capability for detecting ischemia/hypoxia injury. The measurement of sO₂ by PAI achieved an exceptional AUC of 0.997 (95 % CI: 0.894–1.000, Table 2, Fig. 7a). With a cutoff value of 60.9 %, sO₂ measurements yielded a sensitivity of 95 %, specificity of 100 %, and
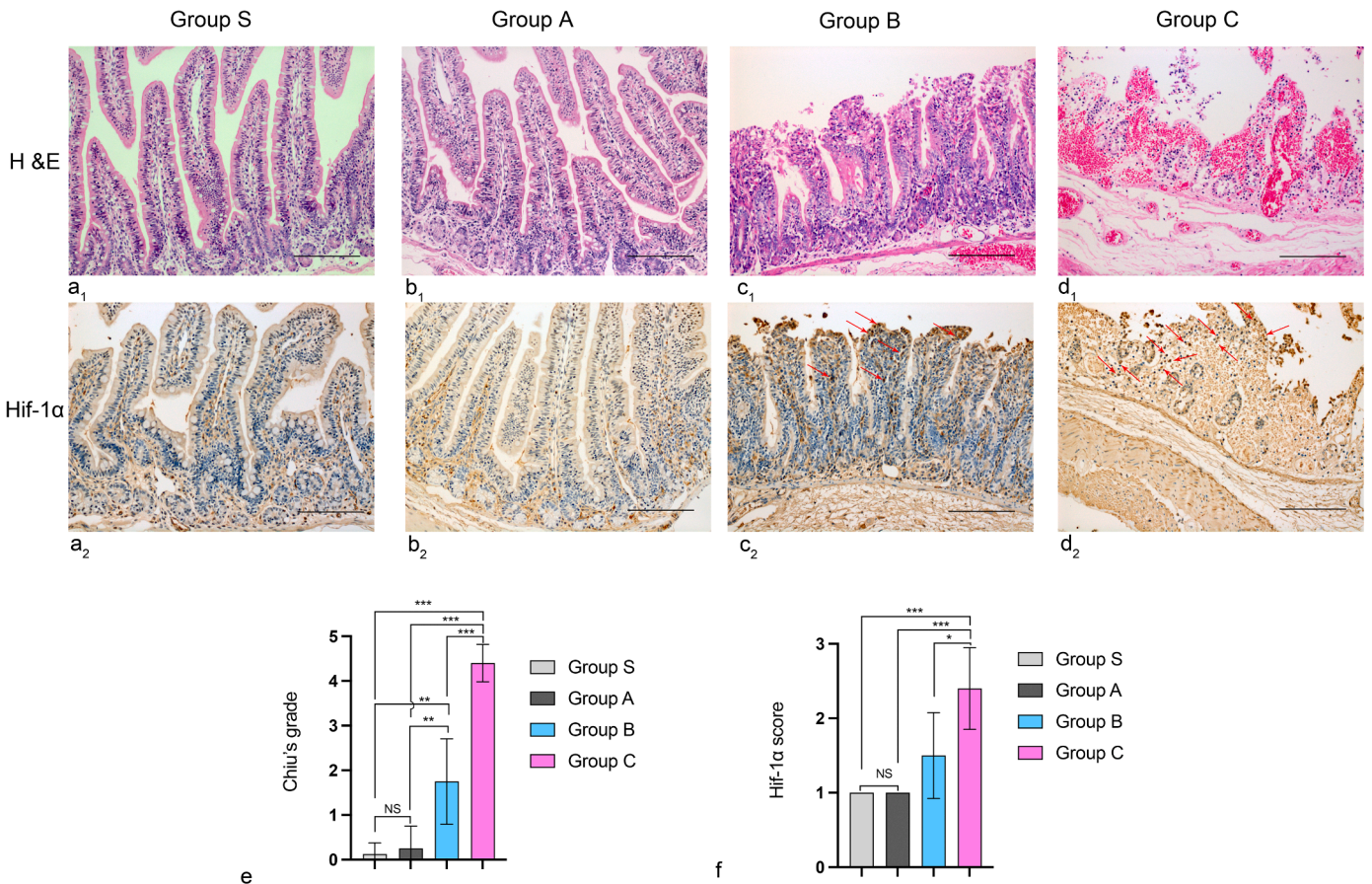
Fig. 5. The histopathological (a_1-d_1) and immunohistochemical (a_2-d_2) analysis of normal intestine and different acute intussusception groups. (a_1-d_1) Representative HE finding of normal intestine or involved intestinal tissue in different groups. (a_2-d_2) Representative Hif-1α staining finding of normal intestine or involved intestinal tissue in different groups. (e) The Chiu's grades results of normal intestine and different acute intussusception groups. (f) The Hif-1α score results of normal intestine and different acute intussusception groups. Red arrows, indicate the Hif-1α staining positive cells. All images were taken at an original magnification of × 200. Scale bar, 200μm. *$P < 0.05$, **$P < 0.01$, ***$P < 0.001$. NS, not significant. Error bar, standard deviation.

Table 2
The diagnostic performance of Alder grade of CDFI, TIC parameters of CEUS and oxygen saturation (sO_2) and HbT counts measured by PAI in identifying ischemia/hypoxia injury of intestine after acute intussusception.

Variable	Cutoff value	AUC[a]	Sensitivity (%)[a]	Specificity (%)[a]	Accuracy (%)
sO_2 (%)	60.9	0.997 (0.894, 1.000)	95 (74, 100)	100 (79, 100)	97
HbT (Counts)	32,314	0.778 (0.600, 0.904)	89 (67, 99)	64 (35, 87)	75
Adler grade	1	0.896 (0.729, 0.977)	89 (65,99)	75 (43, 95)	83
TIC parameters					
AUC (db*s)	725.1	0.939 (0.784, 0.994)	94 (73, 100)	91 (59, 100)	93
PI (db)	20.4	0.864 (0.685, 0.962)	78 (52, 94)	100 (72, 100)	86
TTP (s)	28.2	0.886 (0.713, 0.973)	78 (52, 94)	100 (72, 100)	86
MTT (s)	45.6	0.655 (0.418, 0.845)	50 (19, 81)	91 (59, 100)	71

AUC, area under the curve; CDFI, color Doppler flow imaging; CEUS, contrast-enhanced ultasound; HbT, total hemoglobin; MTT, mean transit time; PAI, photoacoustic imaging; PI, peak intensity; TIC, time-intensity curve; TTP, time to peak.
[a] data in parentheses are 95 % confidence interval.

overall accuracy of 97 % (Table 2). Additionally, HbT counts measured by PAI also showed relatively high diagnostic performance, with an AUC of 0.778 (95 % CI: 0.600–0.904, Table 2, Fig. 7a). Using a threshold of 32,314 counts/mm², HbT measurements achieved a sensitivity of 89 %, specificity of 64 %, and accuracy of 75 % (Table 2). Therefore, intestinal PAI, particularly sO₂, exhibited excellent diagnostic performance in identifying ischemia and hypoxia-related intestinal injury, highlighting its potential for clinical application.

3.6. Diagnostic performance of CDFI, CEUS and PAI in identifying intestinal necrosis after acute intussusception

Regarding the pathological changes that occur after acute intussusception, intestinal necrosis was defined as the Chiu's grade over 4. Based on this classification, the CDFI Adler grade demonstrated moderate diagnostic performance, with an AUC of 0.805 (95 % CI: 0.620–0.926, Table 3, Fig. 6b). While the sensitivity was high at 100 %, the specificity and accuracy were relatively low, at 55 % and 70 %, respectively. Among all the TIC parameters, the AUC of CEUS displayed the highest diagnostic accuracy for intestinal necrosis, achieving an AUC of 0.911
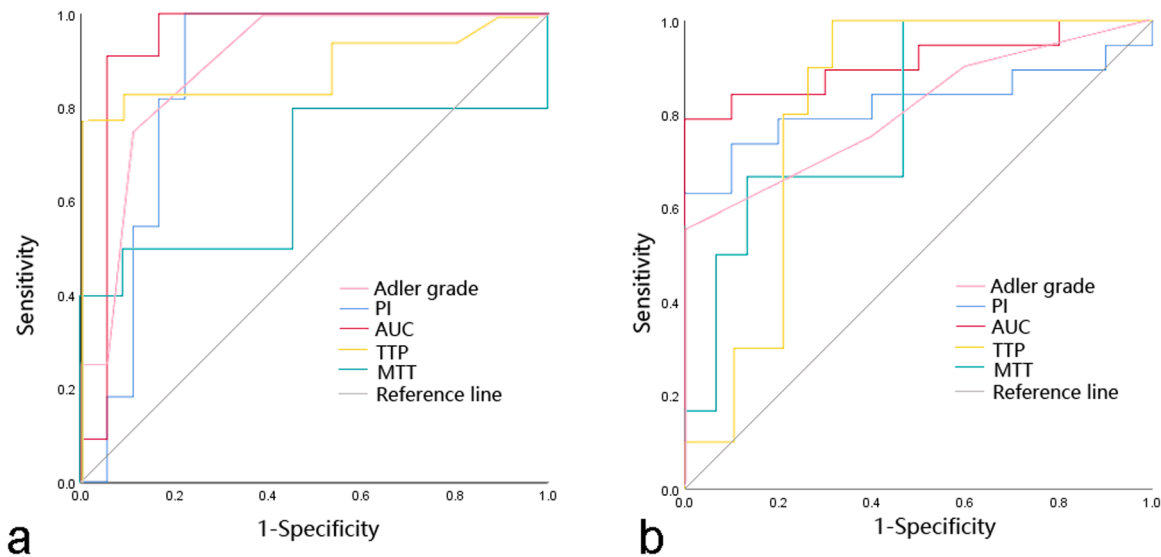
Fig. 6. The receiver operator characteristic (ROC) curve of the Adler grade and time-intensity curve parameters in CEUS. The area under the curves (AUCs) were analyzed for their diagnostic performance in diagnosing ischemia/ hypoxia injury of intestine (a) and intestinal necrosis (b) after acute intussusception. AUC, the area under the curve; CEUS, contrast-enhanced ultrasound; MTT, mean transit time; PI, peak intensity; TTP, time to peak.
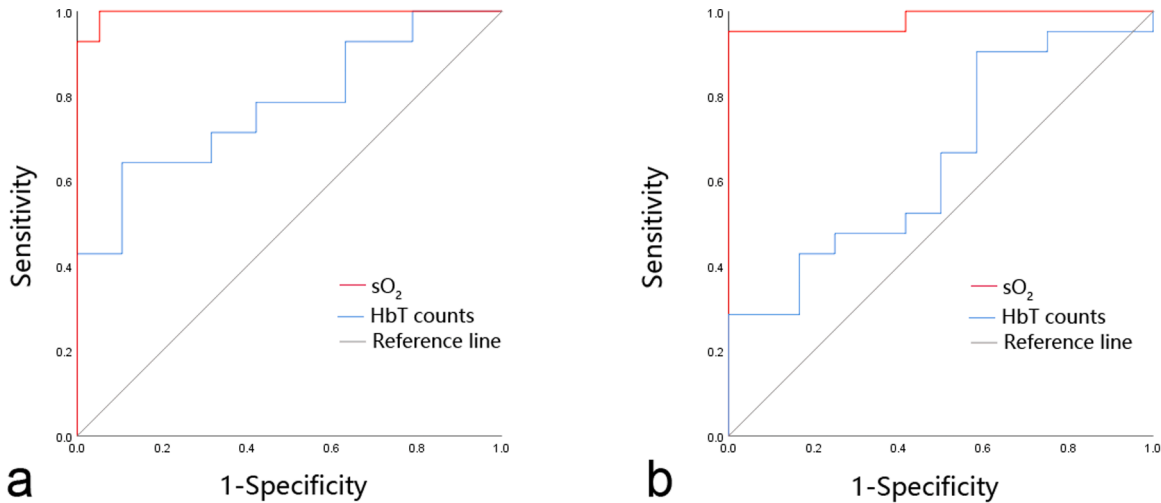

Fig. 7. The receiver operator characteristic (ROC) curve of the oxygen saturation (sO_2) and HbT counts. The area under the curves (AUCs) were analyzed for their diagnostic performance in diagnosing ischemia/ hypoxia injury of intestine (a) and intestinal necrosis (b) after acute intussusception.

Table 3

The diagnostic performance of Alder grade of CDFI, TIC parameters of CEUS and oxygen saturation (sO_2) and HbT counts measured by PAI in identifying intestinal necrosis after acute intussusception.

Variable	Cutoff value	AUC[a]	Sensitivity (%)[a]	Specificity (%)[a]	Accuracy (%)
sO_2 (%)	50.4	0.982 (0.868, 1.000)	100 (74, 100)	95 (78, 100)	98
HbT (Counts)	12,358	0.651 (0.466, 0.808)	42 (15, 72)	90 (70, 99)	59
Adler grade	1	0.805 (0.620, 0.926)	100 (69, 100)	55 (32, 77)	70
TIC parameters					
AUC (db*s)	581.1	0.911 (0.745, 0.984)	100 (69, 100)	79 (54, 94)	86
PI (db)	20.4	0.821 (0.635, 0.938)	90 (56, 100)	74 (49, 91)	79
TTP (s)	23.3	0.816 (0.629, 0.934)	100 (69, 100)	68 (43, 87)	79
MTT (s)	31.3	0.800 (0.570, 0.940)	100 (54, 100)	53 (27, 79)	66

AUC, area under the curve; CDFI, color Doppler flow imaging; CEUS, contrast-enhanced ultrasound; HbT, total hemoglobin; MTT, mean transit time; PAI, photoacoustic imaging; PI, peak intensity; TIC, time-intensity curve; TTP, time to peak.

[a] data in parentheses are 95 % confidence interval.

(95 % CI: 0.745–0.984, Table 3, Fig. 6b), a sensitivity of 100 %, specificity of 79 %, and accuracy of 86 %. These results indicate that CEUS is superior to CDFI in diagnosing intestinal necrosis after acute intussusception.

PAI further demonstrated outstanding performance in diagnosing intestinal necrosis. The sO_2 measurement achieved an exceptional AUC

of 0.982 (95 % CI: 0.868–1.000, Table 3, Fig. 7b). Using a cutoff value of 50.4 %, sO_2 exhibited a sensitivity of 100 %, specificity of 95 %, and overall accuracy of 98 % (Table 3). However, HbT counts measured by PAI demonstrated moderate diagnostic performance, with an AUC of 0.651 (95 % CI: 0.466–0.808, Table 3, Fig. 7b). Using a cutoff value of 12,358 counts/mm^2, HbT measurements showed a relatively high specificity of 90 %; however, sensitivity and accuracy were lower at 42 % and 59 %, respectively (Table 3). Therefore, intestinal sO_2 obtained via PAI demonstrated superior diagnostic performance in identifying intestinal necrosis compared to HbT counts, further underscoring its promise for clinical implementation.

4. Discussion

Acute intussusception is a pediatric abdominal emergency that necessitates immediate diagnosis and appropriate treatment. Accurately identifying bowel necrosis non-invasively is essential for clinical decision-making regarding non-operative reduction or emergency surgery [2]. However, this remains challenging with conventional imaging modalities such as grey-scale sonography or color Doppler flow imaging (CDFI). While the absence of blood flow on CDFI is considered an indicator of enema reduction failure and intestinal necrosis [5–7], our study demonstrated that although CDFI exhibited high sensitivity (100 %), its specificity (55 %) and accuracy (70 %) were relatively low (Table 3). This suggests a risk of misdiagnosing intestinal necrosis, potentially leading to unnecessary exclusion of patients from enema reduction attempts.

In this study, for the first time, we demonstrated that the intestinal sO_2 measurements obtained through PAI exhibited excellent diagnostic performance in identifying ischemia/ hypoxia injury of intestine following acute intussusception with an AUC of 0.997 (Fig. 7a), and high sensitivity, specificity, and accuracy (Table 2). Similarly, PAI-measured intestinal sO_2 exhibited outstanding diagnostic performance in identifying intestine necrosis following acute intussusception with an AUC of 0.982 (Fig. 7b), along with high sensitivity, specificity, and accuracy (Table 3). These findings highlight the potential of PAI for clinical application in guiding appropriate therapeutic strategies.

As a reference standard for assessing blood supply, CEUS enables real-time red blood cell imaging, and has demonstrated high diagnostic performance in identifying both intestinal ischemia/hypoxia and necrosis in our study. Additionally, the probe frequency and imaging depth of CEUS are more aligned with actual clinical scenarios, further supporting its potential for clinical application. In comparison, while PAI-derived sO_2 exhibits strong diagnostic capabilities for detecting intestinal ischemia/ hypoxia and necrosis following acute intussusception, optimization of imaging parameters—such as probe frequency and imaging depth—is necessary to enhance its clinical translation and applicability in preclinical studies [23].

The HbT counts measured by PAI demonstrated moderate diagnostic performance in identifying intestinal ischemia/ hypoxia and necrosis following acute intussusception, with an AUC of 0.778 and 0.651, respectively (Fig. 7a and b), which suggests that HbT counts are less capable to diagnose intestinal ischemia/ hypoxia and necrosis than sO_2. Since HbT counts are derived from the PAI signals of both deoxygenated and oxygenated hemoglobin, and CDFI relies on the Doppler effect, the two modalities may introduce biases between the actual blood supply and the measurement values. In contrast, CEUS utilizes real-time red blood cell imaging, directly depicting blood supply. As a result, CEUS demonstrated higher diagnostic performance in identifying intestinal ischemia/hypoxia and necrosis compared to both HbT counts and CDFI.

Typically, due to blood vessel compression, the intussusceptum (the proximal segment, typically the ileum) is more vulnerable to hypoxia and necrosis than the intussuscipiens (the recipient distal segment, typically the colon) in acute intussusception [24]. Our results support this, as we observed a significant decrease in sO_2 and HbT levels in the intussusceptum two hours after intussusception, while no significant changes in sO_2 and HbT levels were noted in the intussuscipiens (Table 1 and Fig. 3).

PAI is an emerging effective diagnostic imaging modality for assessing intestinal diseases. Weis, V.G. et al. [18] demonstrated that PAI is a valuable non-invasive and quantitative method for assessing intestinal sO_2 in neonatal rats, with their subsequent study [25] showing significant decreases in intestinal sO_2 measured by PAI in neonatal rats with necrotizing enterocolitis. Moreover, PAI is a novel quantitative imaging technique that allows for continuous monitoring of tissue oxygenation, which can guide treatment strategies and surgical decisions. For instance, Sugiura T. et al. [26] showed that PAI could continuously monitor intestinal sO_2 during surgery for acute mesenteric ischemia and predict intestinal viability, potentially preventing inadequate surgeries.

As a hybrid imaging technique, the PAI/US system enables the parallel collection of anatomical and functional information, allowing for the quantification of oxygenation and providing spatially resolved sO_2 and HbT values for specific tissue regions of interest [27]. These capabilities have been applied in the diagnosis, severity evaluation, and activity monitoring of various acute hypoxic/ischemic conditions, such as testicular torsion, as well as inflammatory diseases like Crohn's disease and rheumatoid arthritis [13,14,28,29].

This study has several limitations. Firstly, although the VEVO LAZR PAI system has been widely used in experimental studies[11,14,18,25, 26,30,31], this is the first instance of its application in assessing acute intussusception, leading to potential sampling errors when applied to individual animals in different groups. There may be impact of different skin tone of individual animals on PAI that we did not consider [32]. Secondly, due to the limited measurement depth (approximately 1 cm) of the VEVO LAZR PAI system, we were unable to perform PAI with the abdomen closed. In future studies, we may explore the use of alternative PAI systems to detect sO_2 and HbT values with the abdomen closed. Thirdly, we did not detect the hematocrit values of each group, which may have some impact on the sO_2 measurements [33]. Lastly, the 21 MHz transducer used in this study operates at a higher frequency than what is typically employed in clinical settings. As such, this research serves as a preliminary investigation in animals, and further validation of the results will be necessary in larger animal models and, eventually, in human volunteers.

Despite these limitations, this study represents the first attempt to utilize PAI in the assessment of acute intussusception, in comparison with CDFI and CEUS. We demonstrated that the intestinal sO_2 values obtained by PAI had excellent diagnostic capabilities for both ischemia/ hypoxia injury and intestinal necrosis in acute intussusception. These findings suggest that PAI is a promising non-invasive imaging modality with potential for clinical application.

CRediT authorship contribution statement

Ling Wenwu: Methodology, Investigation, Conceptualization. **Liu Juxian:** Supervision, Methodology, Conceptualization. **Luo Yan:** Supervision, Project administration, Funding acquisition, Conceptualization. **Huang Lin:** Writing – review & editing, Supervision, Software, Methodology, Conceptualization. **Wang Hong:** Investigation, Formal analysis, Data curation. **Gou Zehui:** Writing – original draft, Investigation, Formal analysis, Data curation. **Yan Hualin:** Writing – review & editing, Writing – original draft, Methodology, Investigation, Funding acquisition, Formal analysis, Conceptualization. **Zhu Xiaoxia:** Investigation, Data curation.

Declaration of Competing Interest

The authors declare that they have no known competing financial interests or personal relationships that could have appeared to influence the work reported in this paper.

Acknowledgments

None.

Appendix A. Supporting information

Supplementary data associated with this article can be found in the online version at doi:10.1016/j.pacs.2025.100706.

Data Availability

Data will be made available on request.

References

[1] L.I. Kelley-Quon, L.G. Arthur, R.F. Williams, et al., Management of intussusception in children: a systematic review, J. Pedia Surg. 56 (3) (2021) 587–596.
[2] Y. Ito, I. Kusakawa, Y. Murata, et al., Japanese guidelines for the management of intussusception in children, 2011, Pedia Int. 54 (6) (2012) 948–958.
[3] V. di Giacomo, M. Trinci, G. van der Byl, et al., Ultrasound in newborns and children suffering from non-traumatic acute abdominal pain: imaging with clinical and surgical correlation, J. Ultrasound 18 (4) (2015) 385–393.
[4] K.R. Bergmann, A.C. Arroyo, M.O. Tessaro, et al., Diagnostic accuracy of point-of-care ultrasound for intussusception: a multicenter, noninferiority study of paired diagnostic tests, Ann. Emerg. Med. 78 (5) (2021) 606–615.
[5] M.S. Kong, H.F. Wong, S.L. Lin, et al., Factors related to detection of blood flow by color Doppler ultrasonography in intussusception, J. Ultrasound Med. 16 (2) (1997) 141–144.
[6] A.S. Gondek, L. Riaza, D. Cuadras, et al., Ileocolic intussusception: Predicting the probability of success of ultrasound guided saline enema from clinical and sonographic data, J. Pedia Surg. 53 (4) (2018) 599–604.
[7] S. Hanquinet, M. Anooshiravani, A. Vunda, et al., Reliability of color Doppler and power Doppler sonography in the evaluation of intussuscepted bowel viability, Pedia Surg. Int. 13 (5-6) (1998) 360–362.
[8] G. del-Pozo, J. Gonzalez-Spinola, B. Gomez-Anson, et al., Intussusception: trapped peritoneal fluid detected with US–relationship to reducibility and ischemia, Radiology 201 (2) (1996) 379–383.
[9] A.A. Davar, M. Khalili, A. Mashhadi, et al., Risk factors of nonsurgical management failure in pediatric intussusception patients with delayed presentation, Pedia Emerg. Care 38 (12) (2022) 650–653.
[10] P.H. Kim, J. Hwang, H.M. Yoon, et al., Predictors of failed enema reduction in children with intussusception: a systematic review and meta-analysis, Eur. Radio. 31 (11) (2021) 8081–8097.
[11] M.M. Menger, C. Korbel, D. Bauer, et al., Photoacoustic imaging for the study of oxygen saturation and total hemoglobin in bone healing and non-union formation, Photoacoustics 28 (2022) 100409.
[12] F. Knieling, C. Neufert, A. Hartmann, et al., Multispectral optoacoustic tomography for assessment of crohn's disease activity, N. Engl. J. Med. 376 (13) (2017) 1292–1294.
[13] A.P. Regensburger, M. Eckstein, M. Wetzl, et al., Multispectral optoacoustic tomography enables assessment of disease activity in paediatric inflammatory bowel disease, Photoacoustics 35 (2024) 100578.
[14] Q. Yang, L. Yang, C. Peng, et al., Testicular torsion diagnosis and injury assessment using photoacoustic oxygenation imaging, Photoacoustics 31 (2023) 100499.
[15] A. Patel, R.N. Kaleya, R.J. Sammartano, Pathophysiology of mesenteric ischemia, Surg. Clin. North Am. 72 (1) (1992) 31–41.
[16] M.J. Wu, M. Chen, S. Sang, et al., Protective effects of hydrogen rich water on the intestinal ischemia/reperfusion injury due to intestinal intussusception in a rat model, Med Gas. Res. 7 (2) (2017) 101–106.
[17] D.D. Adler, P.L. Carson, J.M. Rubin, et al., Doppler ultrasound color flow imaging in the study of breast cancer: preliminary findings, Ultrasound Med. Biol. 16 (6) (1990) 553–559.
[18] V.G. Weis, N. Cruz-Diaz, J.L. Rauh, et al., Photoacoustic imaging as a novel non-invasive biomarker to assess intestinal tissue oxygenation and motility in neonatal rats, J. Pedia Surg. 59 (3) (2024) 528–536.
[19] G. Huang, J. Lv, Y. He, et al., In vivo quantitative photoacoustic evaluation of the liver and kidney pathology in tyrosinemia, Photoacoustics 28 (2022) 100410.
[20] I. Flessas, I. Bramis, E. Menenakos, et al., Effects of lazaroid U-74389G on intestinal ischemia and reperfusion injury in porcine experimental model, Int J. Surg. 13 (2015) 42–48.
[21] J.S. Quaedackers, R.J. Beuk, L. Bennet, et al., An evaluation of methods for grading histologic injury following ischemia/reperfusion of the small bowel, Transpl. Proc. 32 (6) (2000) 1307–1310.
[22] J.E. Ziello, I.S. Jovin, Y. Huang, Hypoxia-Inducible Factor (HIF)-1 regulatory pathway and its potential for therapeutic intervention in malignancy and ischemia, Yale J. Biol. Med. 80 (2) (2007) 51–60.
[23] J. Park, S. Choi, F. Knieling, et al., Clinical translation of photoacoustic imaging, Nat. Rev. Bioeng. (2024) 1–20.
[24] M. Waseem, H.K. Rosenberg, Intussusception, Pedia Emerg. Care 24 (11) (2008) 793–800.
[25] J.A. Weis, J.L. Rauh, M.A. Ellison, et al., Photoacoustic imaging for non-invasive assessment of biomarkers of intestinal injury in experimental necrotizing enterocolitis, Pedia Res. (2024).
[26] T. Sugiura, K. Okumura, J. Matsumoto, et al., Predicting intestinal viability by consecutive photoacoustic monitoring of oxygenation recovery after reperfusion in acute mesenteric ischemia in rats, Sci. Rep. 11 (1) (2021) 19474.
[27] W. Choi, E.Y. Park, S. Jeon, et al., Three-dimensional Multistructural Quantitative Photoacoustic and US Imaging of Human Feet in Vivo, Radiology 303 (2) (2022) 467–473.
[28] K. Tascilar, F. Fagni, A. Kleyer, et al., Non-invasive metabolic profiling of inflammation in joints and entheses by multispectral optoacoustic tomography, Rheumatol. (Oxf.) 62 (2) (2023) 841–849.
[29] M. Yang, C. Zhao, M. Wang, et al., Synovial oxygenation at photoacoustic imaging to assess rheumatoid arthritis disease activity, Radiology 306 (1) (2023) 220–228.
[30] M. Zhou, L. Zhang, J. Zeng, et al., Visualizing the early-stage testicular torsion by dual-modal photoacoustic and ultrasound imaging, Photoacoustics 31 (2023) 100523.
[31] A.V. Nikolaev, Y. Fang, J. Essers, et al., Pre-transplant kidney quality evaluation using photoacoustic imaging during normothermic machine perfusion, Photoacoustics 36 (2024) 100596.
[32] Y. Mantri, J.V. Jokerst, Impact of skin tone on photoacoustic oximetry and tools to minimize bias, Biomed. Opt. Express 13 (2) (2022) 875–887.
[33] S. Paul, H.S. Patel, R.K. Saha, Quantitative evaluation of the impact of variation of optical parameters on the estimation of blood hematocrit and oxygen saturation for dual-wavelength photoacoustics, J. Opt. Soc. Am. A Opt. Image Sci. Vis 41 (6) (2024) 1128–1139.

Hualin Yan is currently a doctor in Department of Ultrasound, West China Hospital, Sichuan University. He completed joint training PhD program in Boston Children's Hospital/Harvard Medical School in 2017 and received his Ph.D. degree in 2018 from Sichuan University. He completed the post-doctoral fellowship in Sichuan University in 2021. His research mainly focuses on pediatric ultrasonography and the clinical application of photoacoustic imaging.
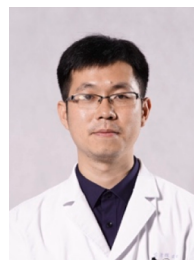
Zehui Gou is an attending physician in Department of Ultrasound, West China Hospital, Sichuan University. He got his Master's degree from Sichuan University in 2019. He has worked in the field of clinical imaging, especially in interventional ultrasound.

Hong Wang is currently an ultrasound technician in Department of Ultrasound, West China Hospital, Sichuan University. She received her Master's degree in 2018 from Sichuan University. Her research mainly focuses on the clinical application of new ultrasound imaging technology.

Xiaoxia Zhu is a research assistant of West China Hospital, Sichuan University. She received her Master's degree in 2012 from Southwest Minzu University with expertise in Veterinary Medicine.

Lin Huang received the Ph.D. degree in optics from the University of Electronic Science and Technology, Chengdu, China, in 2015. He is currently an Associate Professor with the University of Electronic Science and Technology of China. His research is focused on discovering and developing fundamentally electromagnetic related imaging technologies for in vivo visualization of tissue at both the macroscopic and microscopic scales.

Juxian Liu is an associate professor in Department of Ultrasound, West China Hospital, Sichuan University. She received her Master's degree in 2007 from Sichuan University and visited Prince of Wales Hospital, The Chinese University of Hong Kong in 2007 as a research assistant. Her research mainly focuses on the ultrasound diagnosis of abdominal, superficial, musculoskeletal, and peripheral nerve disorders in children.

Yan Luo is currently the department director and a Professor of Department of Ultrasound, West China Hospital, Sichuan University. She has been engaged in clinical and scientific research in ultrasound. Her current research interests include ultrasonography for abdominal diseases (especially liver diseases) and emerging imaging technologies.

Wenwu Ling is the vice director and associate professor of Department of Ultrasound, West China Hospital, Sichuan University. He graduated from Sichuan University in 2019 with Ph. D. degree. He has been engaged in clinical and scientific research in ultrasound. His research mainly focuses on the contrast-enhanced ultrasound and elastography of abdominal diseases.